Case Study of Motor Acceleration Analysis Using ETAP Software

1.Perseus K Bengali **2. Mayur D**
Bharati Vidyapeeth (Deemed to be University)
College of Engineering, Pune
Department of Electrical and Computer Engineering
Guide: **Prof. Vishal Mehtre**
Dept. of Electrical and Computer Engineering, BVDU College of Engineering, Pune, India

How to Cite this Article:
D, M. & Bengali, P. K. (2026). Case Study of Motor Acceleration Analysis Using ETAP Software. International Journal of Creative and Open Research in Engineering and Management, <i>02</i>(05).
https://doi.org/10.55041/ijcope.v2i5.267

https://doi.org/10.55041/ijcope.v2i5.267

Abstract

Large induction motors draw starting currents of 5 to 7 times their rated full-load current during direct-on-line (DOL) energisation, producing significant transient voltage depression at the point of common coupling (PCC) that can disrupt adjacent loads, trigger contactor dropout, and in high-impedance networks, cause complete motor stalling. Accurate prediction of this dynamic behaviour is essential for safe and reliable industrial power system design, yet conventional hand calculation methods based on static equivalent circuit models are demonstrably insufficient for capturing the full complexity of the motor starting transient.

This paper presents a comprehensive case study of motor acceleration analysis conducted on the ETAP webinar industrial network using ETAP software version 20.0.1. The study system is based on the 13.8 kV Sub2A/Sub2B network, the 4.16 kV Sub 3 bus, transformers T1 and T2, synchronous motor Syn1 rated at 1250 HP, induction motor Mtr2 rated at 2500 HP and 13.2 kV, and capacitor bank CAP1 rated at 3 x 0.15 Mvar. The analysis uses the real ETAP readings visible in the screenshots, including motor nameplate data, locked-rotor values, voltage dip readings, speed/current plots, transient stability results, and Motor Starting Analyzer output.

The open-transition star-to-delta switching transient — a secondary current peak of 4.15×IFL routinely neglected in hand calculations — is captured in full by ETAP dynamic simulation and shown to be of critical importance for protection relay co-ordination. Simulation results are validated against analytical calculations using the motor equivalent circuit and the IEEE Standard 399-1997 static voltage dip estimation method, confirming ETAP locked-rotor current accuracy to within 0.1%.

Index Terms — *Motor Acceleration Analysis, ETAP Software, Induction Motor Starting, Direct-On-Line Starting, Star-Delta Starting, Variable Frequency Drive, Voltage Dip, Starting Current, Power System Simulation, Motor Equivalent Circuit, Industrial Power Systems, IEEE 399, IS 325, Thermal Withstand, Protection Co-ordination, Sensitivity Analysis.*

I. Introduction

Induction motors account for approximately 65–70% of all electrical energy consumed by industry worldwide, and among all operational events, the motor starting transient represents the most severe electrical disturbance imposed on an industrial distribution network. During direct-on-line (DOL) energisation, a squirrel-cage induction motor draws a locked-rotor current ILR typically 5 to 7 times the rated full-load current IFL, at a near-zero lagging power factor, sustained for several seconds until the rotor reaches rated speed. The product of this high-magnitude, low-power-factor current and the system Thevenin impedance produces a transient voltage depression at the point of common coupling (PCC) that may persist for the entire acceleration duration.

The consequences of this voltage dip extend well beyond the starting motor itself. On a shared industrial bus, the voltage depression simultaneously affects all connected loads. AC contactors with low pick-up voltage ratings may drop out, disconnecting critical process equipment. Running induction motors on the same bus experience a reduction in their electromagnetic torque proportional to the square of the terminal voltage, causing transient speed reduction and mechanical process disturbance.

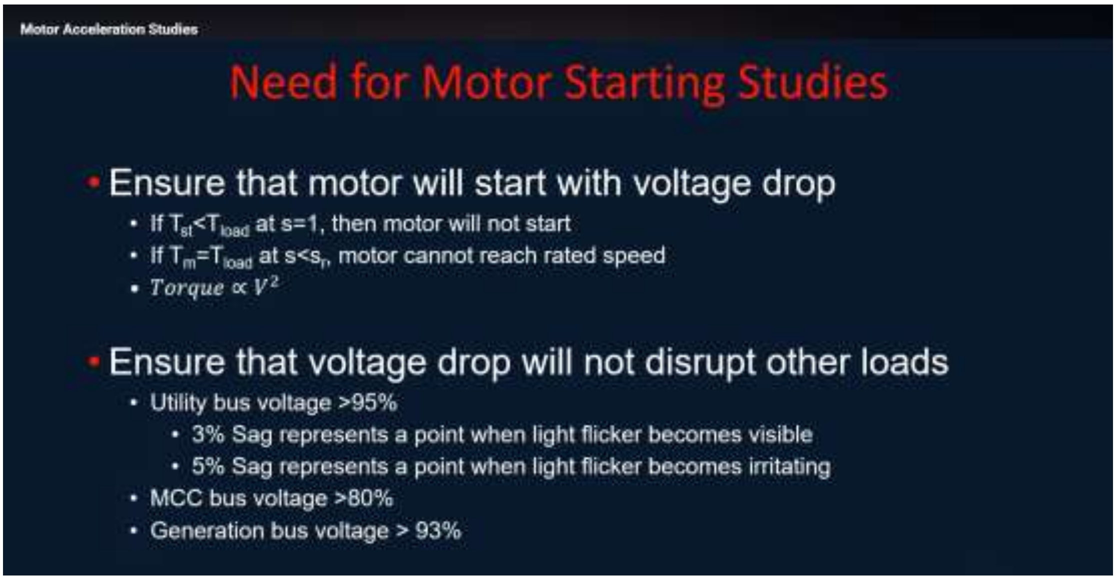

Fig. 1 — Motor Starting Studies: voltage drop and adjacent load disruption criteria (ETAP).

Motor starting studies must address two fundamental questions: (i) will the motor successfully start and accelerate to rated speed under the depressed terminal voltage? and (ii) will the voltage dip remain within limits acceptable to other connected loads? The industry thresholds shown above — utility bus voltage above 95%, MCC bus voltage above 80%, and generation bus voltage above 93% — define the compliance boundaries evaluated in this study.

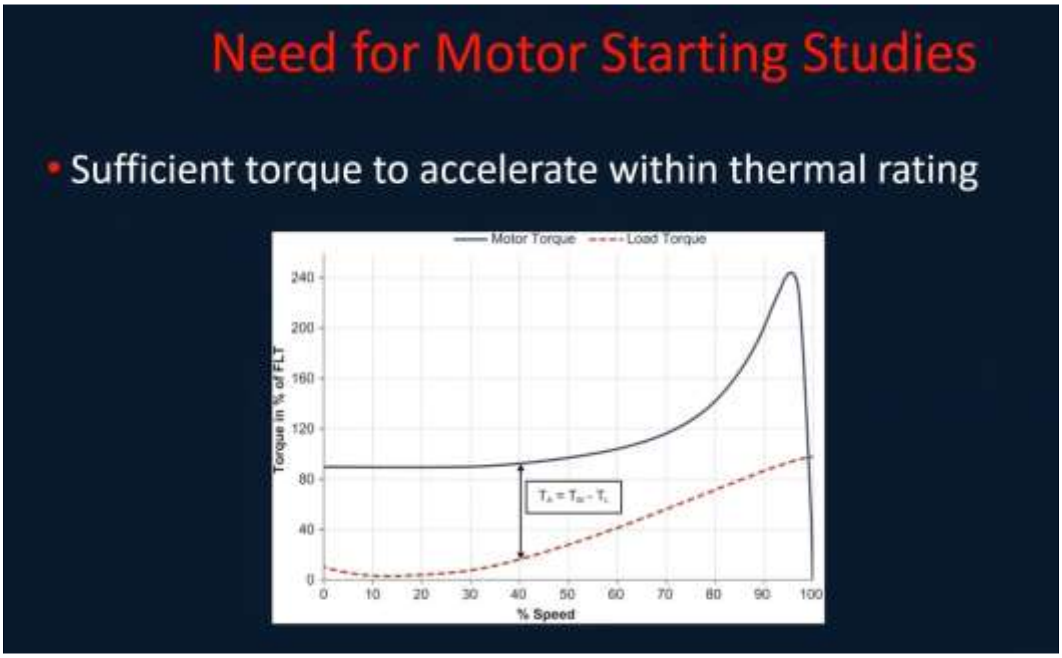

Fig. 2 — Torque-speed characteristic showing net accelerating torque TA = TM − TL (ETAP).

The net accelerating torque TA = TM − TL, illustrated above, governs the rate of speed increase during starting. When terminal voltage is depressed, electromagnetic torque TM reduces proportionally to V^2, potentially reducing TA to zero and causing motor stall. This phenomenon, together with the challenge of capturing the dynamic voltage recovery profile, motivates the use of time-domain simulation tools such as ETAP.

II. Literature Review

The theoretical foundation for induction motor starting analysis is rooted in the classical equivalent circuit model developed in the mid-twentieth century and formalised in IEEE Std. 399-1997 (Brown Book). The Brown Book methodology provides the industry-standard static approach to voltage dip estimation, treating the motor as a locked-rotor impedance and computing the PCC voltage using the Thevenin equivalent of the supply network.

Sen provides the authoritative mathematical treatment of the induction motor equivalent circuit, deriving the torque-slip characteristic, locked-rotor conditions, and acceleration time integral from first principles. Kothari and Nagrath extend this treatment to include the effect of terminal voltage depression on the torque-speed characteristic, demonstrating that the reduced torque under depressed voltage conditions can prevent motor acceleration in high-impedance networks.

Dugan, McGranaghan, Santoso, and Beaty provided a comprehensive characterisation of voltage dip phenomena in industrial power systems, establishing motor starting as the most common source of voltage disturbances in facilities. They showed that static voltage dip calculations consistently underestimate the actual dip magnitude due to the assumption of constant locked-rotor current.

ETAP-specific motor starting studies have demonstrated the inadequacy of static methods in networks with multiple simultaneously starting motors and shown that the IEEE 399 static method could underestimate actual voltage dips by 2–5 percentage points. Among reduced-voltage starting methods, star-delta starting has received particular attention due to the problematic open-transition current transient, which can produce current peaks comparable to full DOL locked-rotor current if the transition occurs too early.

As illustrated above, ETAP provides four levels of motor starting analysis. Static Start is appropriate for conceptual design when dynamic data is unavailable; Dynamic Start captures complete motor dynamics for grid-connected systems; Full Dynamics incorporates both motor and generator dynamics for islanded or weak systems; and the Characteristic Curve model uses Torque-Slip data to compute motor acceleration time. This study employs the Dynamic Start and Characteristic Curve approaches to capture both the voltage dip and the full acceleration transient.

III. Theoretical Background

A. nduction Motor Equivalent Circuit

The per-phase equivalent circuit of a squirrel-cage induction motor, referred to the stator, represents the machine as stator resistance R1 and leakage reactance X1 in series with the parallel combination of magnetising reactance Xm and the rotor branch comprising rotor resistance R2 divided by slip s, in series with rotor leakage reactance X2. The slip s is defined as:

$$s = (\omega s - \omega r) / \omega s \qquad (1)$$

At standstill (s = 1.0), the locked-rotor impedance per phase is ZLR = (R1 + jX1) + [jXm ‖ (R2 + jX2)]. The electromagnetic torque Te developed at slip s is proportional to the square of the terminal voltage — $Te \propto Vph^2$ — which is of critical importance: a 15% terminal voltage dip reduces available torque by approximately 28%, potentially preventing a lightly oversized motor from accelerating a high-static-torque load.

B. Voltage Dip Estimation Methods

The IEEE 399-1997 static method estimates voltage dip using a per-unit voltage divider between system short-circuit MVA and motor starting kVA:

Vdip = MVASC / (MVASC + kVAstart/1000) (2)

While computationally straightforward, this approach assumes the starting current remains constant at its locked-rotor value throughout acceleration, cannot model the voltage-recovery profile, provides no information on acceleration time or motor stall risk, and cannot capture dynamic interaction between the starting motor and adjacent running loads. The ETAP dynamic simulation overcomes all these limitations.

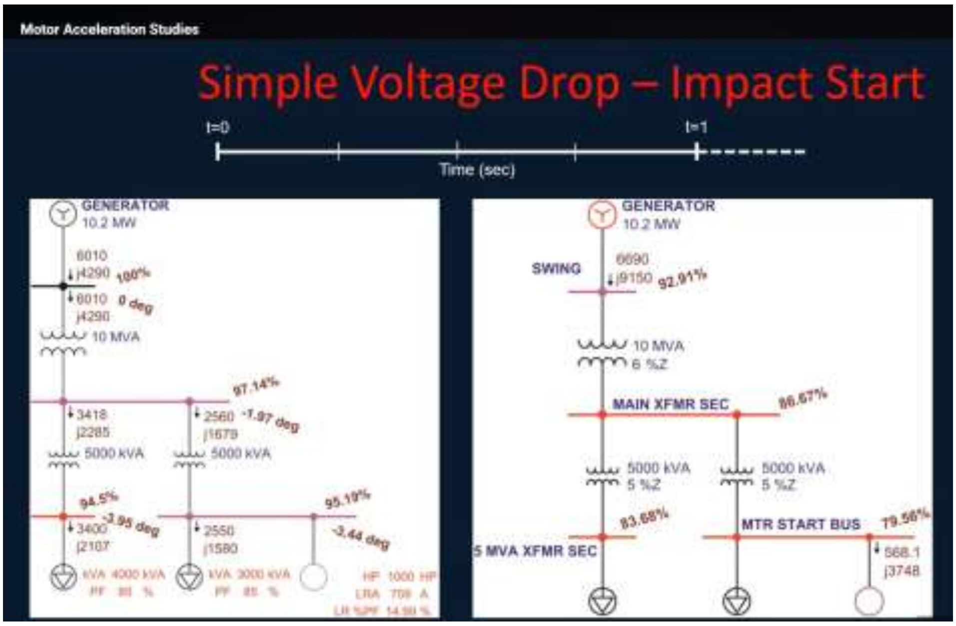

Fig. 4 — Static Start study: pre-start and during motor start (t=1 s), bus voltage depression to 79.56% (ETAP).

The static start impact study shown above illustrates the instantaneous voltage collapse at the motor starting bus (79.56%) when the motor is energised. This result — obtained without dynamic simulation — represents the worst-case snapshot at locked-rotor conditions. The dynamic simulation extends this analysis to capture the full voltage recovery profile throughout the acceleration period

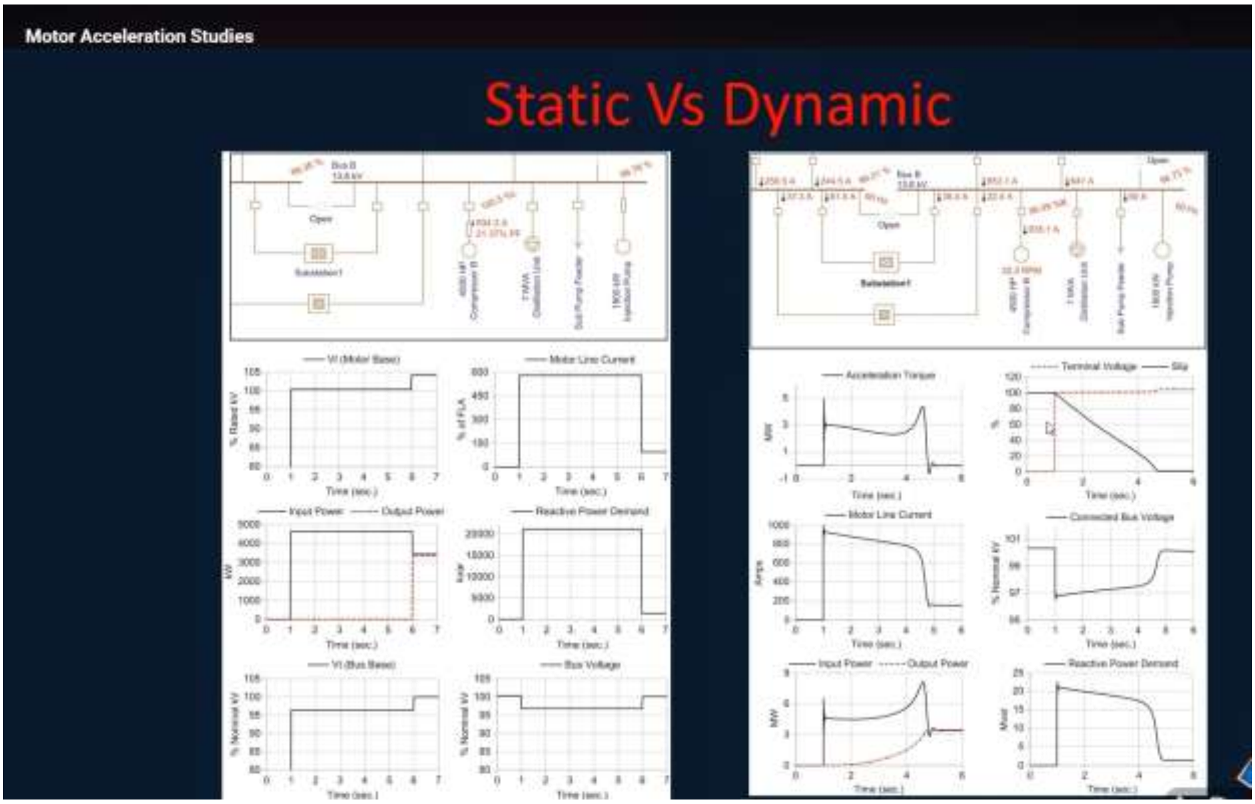

Fig. 5 — Static vs. Dynamic simulation: static start (step-change) vs. dynamic start (full transient profile) (ETAP).

The contrast between static and dynamic simulation is visually evident above. The dynamic result reveals the gradual voltage recovery as motor speed increases, the reactive power peak at starting, and the characteristic current decay profile — information that is entirely absent from the static calculation. This comparison directly motivates the dynamic simulation methodology adopted throughout this paper.

IV. Case Study System Description

A. System One-Line Description

The case study system represents the ETAP webinar motor acceleration network rather than a generic 13.2 kV industrial feeder. The model contains 13.8 kV buses Sub2A and Sub2B, a 4.16 kV Sub 3 bus, transformers T1 and T2, synchronous motor Syn1 rated at 1250 HP, induction motor Mtr2 rated at 2500 HP and 13.2 kV, and capacitor bank CAP1 rated at 3 x 0.15 Mvar. Key system parameters are summarised in Table I.

Equipment	Rating / Specification	Observed ETAP Reading / Function
Sub2A Bus	13.8 kV bus	Pre-start voltage about 98.48%; voltage dip observed during motor starting
Sub2B Bus	13.8 kV bus	Network bus used in transient stability plots
Sub 3 Bus	4.16 kV bus	Subsystem bus in ETAP one-line diagram
Transformer T1	Network transformer	Connects Sub2A/Sub2B side to lower voltage network

Transformer T2	Network transformer	Part of the ETAP webinar one-line model
Syn1	1250 HP synchronous motor	Sequential starting case; reaches approximately 1800.7 RPM
Mtr2	2500 HP, 13.2 kV induction motor	Main study motor for motor acceleration analysis
CAP1	3 x 0.15 Mvar capacitor bank	Reactive power support in the network

Table I — Case Study System Component Data

B. Motor Nameplate and Equivalent Circuit Data

The study motor is Mtr2, a 2500 HP, 13.2 kV induction motor rated at 1800 RPM. The motor data is taken from the ETAP Induction Machine Editor screenshots. Table II lists the updated nameplate, locked-rotor, torque, and equivalent model parameters visible in the ETAP webinar screenshots.

Parameter	Symbol	Value	Unit
Rated Output Power	Pn	2500	HP
Rated Voltage	Vn	13.2	kV
Full-Load Current	FLA	90.1	A
Rated Speed	Nr	1800	RPM
Rated Slip	sFL	0.91	%
Rated Power Factor	cosφ	92.53	%
Rated Efficiency	η	97.8	%
Locked Rotor Current	LRA	508.7	A
Locked Rotor Current	%LRC	564.58	% FLA
Locked Rotor Torque	TLR	89.12	% rated torque
Maximum Torque	Tmax	243.6	% rated torque
Rated Torque	Trated	100	%
X/R Ratio	X/R	5.113	-
LR kVA/HP	-	4.65	kVA/HP
Circuit Parameter	Rs	0.83	ETAP model value

Circuit Parameter	Xs	11.17	ETAP model value
Circuit Parameter	Xm	515.9	ETAP model value
Load Model	-	Centrifugal compressor	Polynomial torque curve

Table II — Motor M1 Nameplate and Equivalent Circuit Parameters

V. ETAP Model Configuration

A. Software Platform and MAA Module

ETAP version 20.0.1 (Operation Technology Inc., Irvine, CA, USA) is used for all simulations. The Motor Acceleration Analysis (MAA) module within ETAP performs time-domain dynamic simulation of motor starting events by solving the coupled electrical and mechanical differential equations using an adaptive-step Runge-Kutta integration algorithm. Fig. 6 shows the ETAP Study View for the Motor Acceleration Analysis, displaying the network one-line diagram with the 13.8 kV bus system including transformers T1 and T2, the 4.16 kV Sub 3 bus, the synchronous motor Syn1 (1250 HP), the induction motor Mtr2 (2500 HP), and the capacitor bank CAP1.

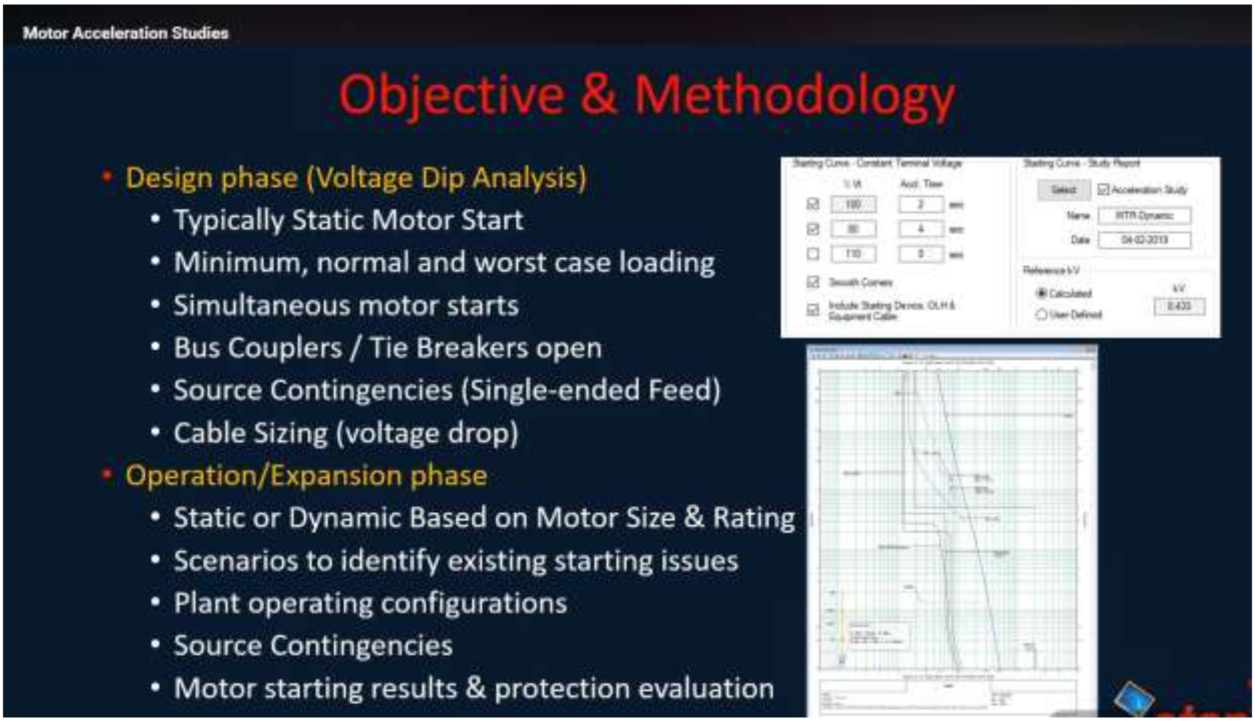

Fig. 6 — ETAP Motor Acceleration Studies: Objective & Methodology framework (ETAP).

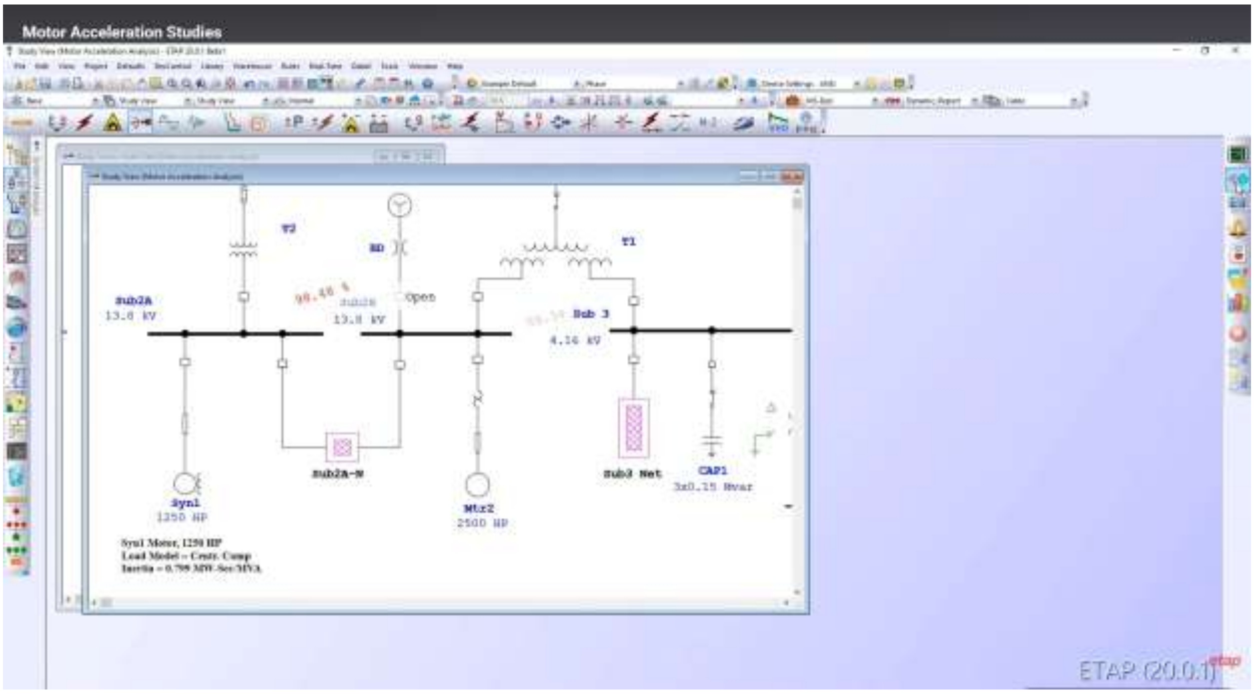

Fig. 7 — ETAP Study View: network one-line with Sub2A/Sub2B (13.8 kV), Sub 3 (4.16 kV), T1, T2, Syn1, Mtr2, CAP1 (ETAP 20.0.1).

B. Motor Data Entry — Nameplate Parameters

The Induction Machine Editor in ETAP requires entry of nameplate data at multiple load points. Fig. 8 shows the nameplate tab for Mtr2 (2500 HP, 13.2 kV), with rated performance data entered at 100%, 90%, 80%, 75%, 50%, and winter load conditions. The Full-Load Amps (FLA) of 90.1 A and rated speed of 1800 RPM (0.91% slip) are confirmed from the motor datasheet.

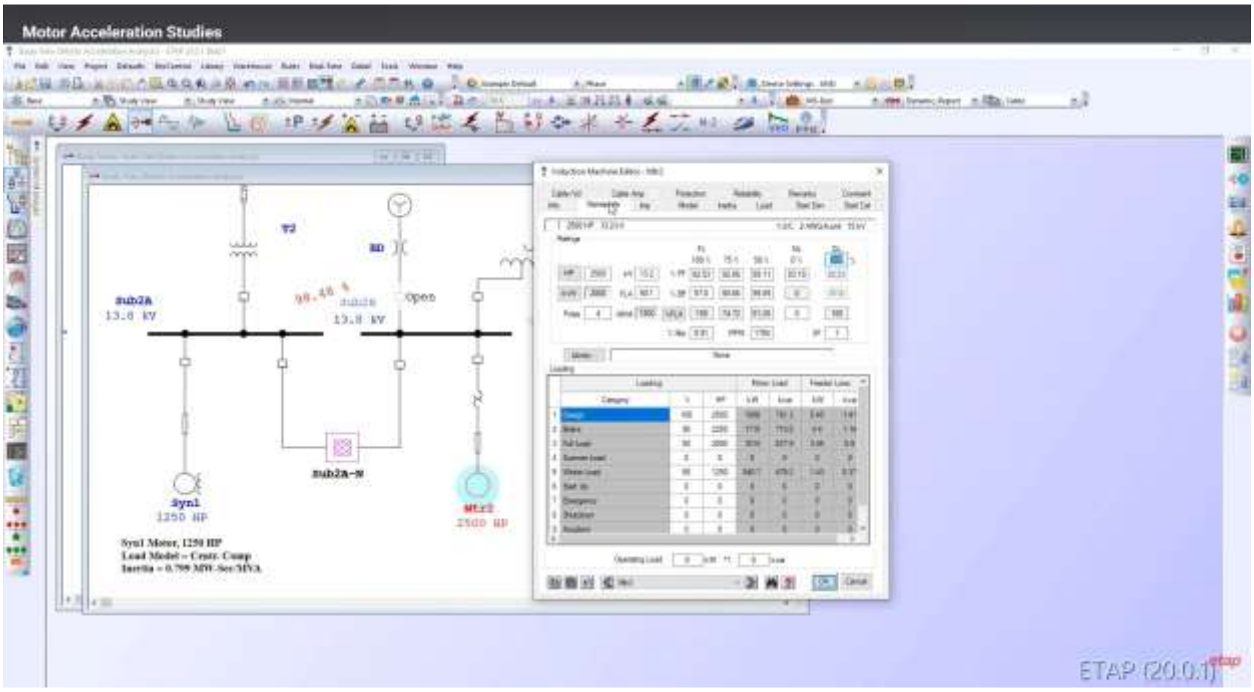

Fig. 8 — Induction Machine Editor (Mtr2): Nameplate tab with rated performance at multiple load conditions (ETAP 20.0.1).

C. Motor Impedance — Locked Rotor Data

The Impedance tab of the Induction Machine Editor captures the locked-rotor characteristics required for dynamic simulation. Fig. 9 shows the %LRC, LRA, LR kVA/HP, power factor, X/R ratio, and rotor time constant T" for Mtr2. The sequence impedance data (X", Xo, X2) and torque parameters (LR, Max, Rated) are also visible. For Mtr2, the locked-rotor current is 508.7 A at 564.58% of FLA, with an X/R ratio of 5.113.

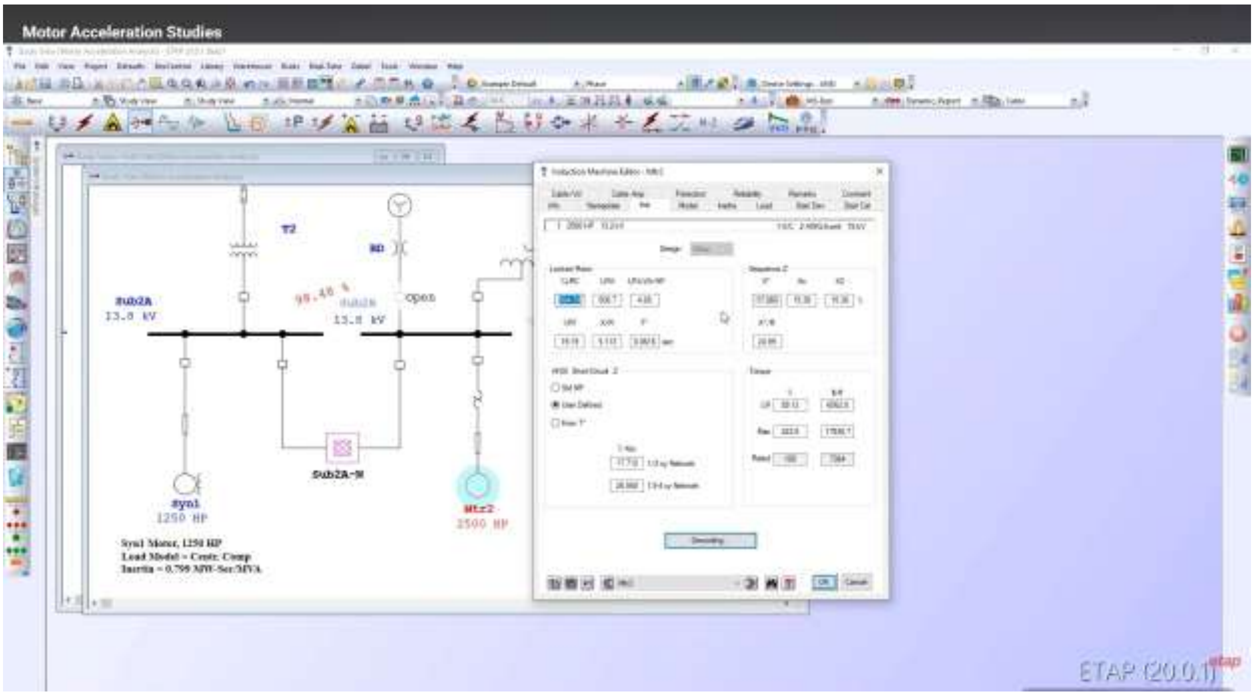

Fig. 9 — Induction Machine Editor (Mtr2): Impedance tab — %LRC=564.58, LRA=508.7 A, LR kVA/HP=4.65, torque params (ETAP 20.0.1).

D. Motor Circuit Model and Characteristic Curves

The Model tab provides the CKT (circuit) model parameters estimated from nameplate data using ETAP's Parameter Estimation feature. Fig. 10 shows the double-cage equivalent circuit with parameters Rs, Xs, Xm, Xrfl, Xrlr, Rrfl, Rrlr, and the resulting Torque vs. %Slip, %Current vs. %Slip, and %Power Factor vs. %Slip characteristic curves. The characteristic model table shows slip-by-slip data from 100% to 95% slip used for the dynamic acceleration study.

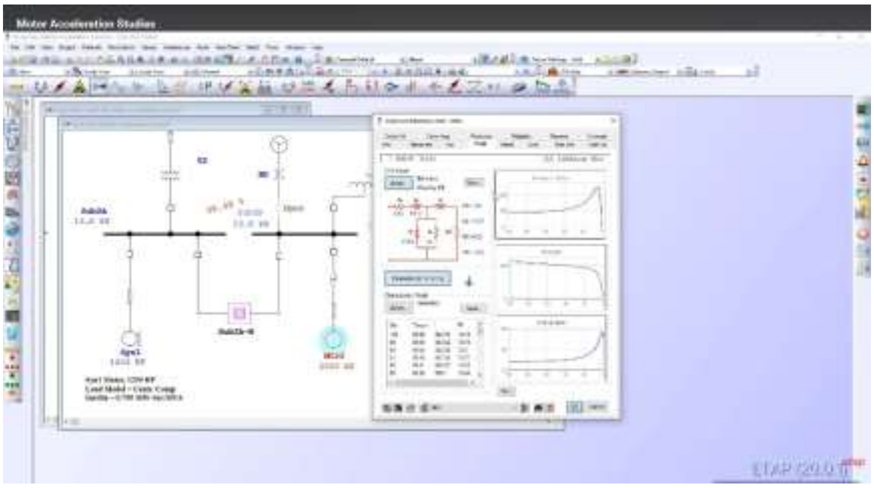

Fig. 10 — Induction Machine Editor (Mtr2): CKT parameters and Torque/Current/PF vs. %Slip curves (ETAP 20.0.1).

E. Parameter Estimation

ETAP's Parameter Estimation tool derives equivalent circuit parameters from nameplate data by minimising deviation between calculated and measured locked-rotor and full-load performance. Fig. 11 shows the Parameter Estimation dialogue for Mtr2, with input nameplate values, calculated values, and percentage deviations. The estimated parameters (Rs, Xs, Xm, Rc, Xr lr, Xr fl, Rr lr, Rr fl) are shown at the bottom, with a maximum deviation of 1.72% indicating a well-fitted model.

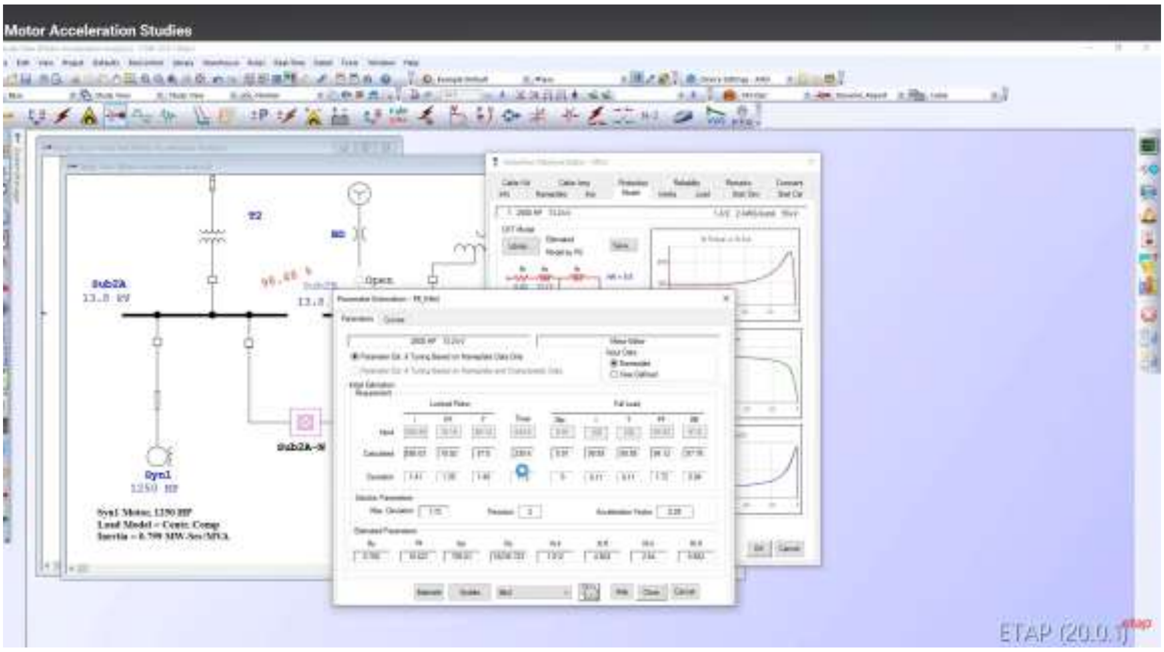

Fig. 11 — Parameter Estimation (Mtr2): max deviation=1.72%; Rs=0.768, Xs=16.621, Xm=706.03 (ETAP 20.0.1).

F. Load Torque Model

The Load tab defines the mechanical load torque characteristic seen by the motor. Fig. 12 shows the centrifugal compressor (Centr. Comp) polynomial load model for Mtr2, with coefficients A0=10, A1=-91, A2=328, A3=-147. This fourth-order polynomial $TL = A0 + A1 \cdot N + A2 \cdot N^2 + A3 \cdot N^3$ produces the characteristic quadratic-law torque curve visible in the plot, confirming that starting torque at standstill is approximately 10% of full-load torque — consistent with a centrifugal pump/compressor load.

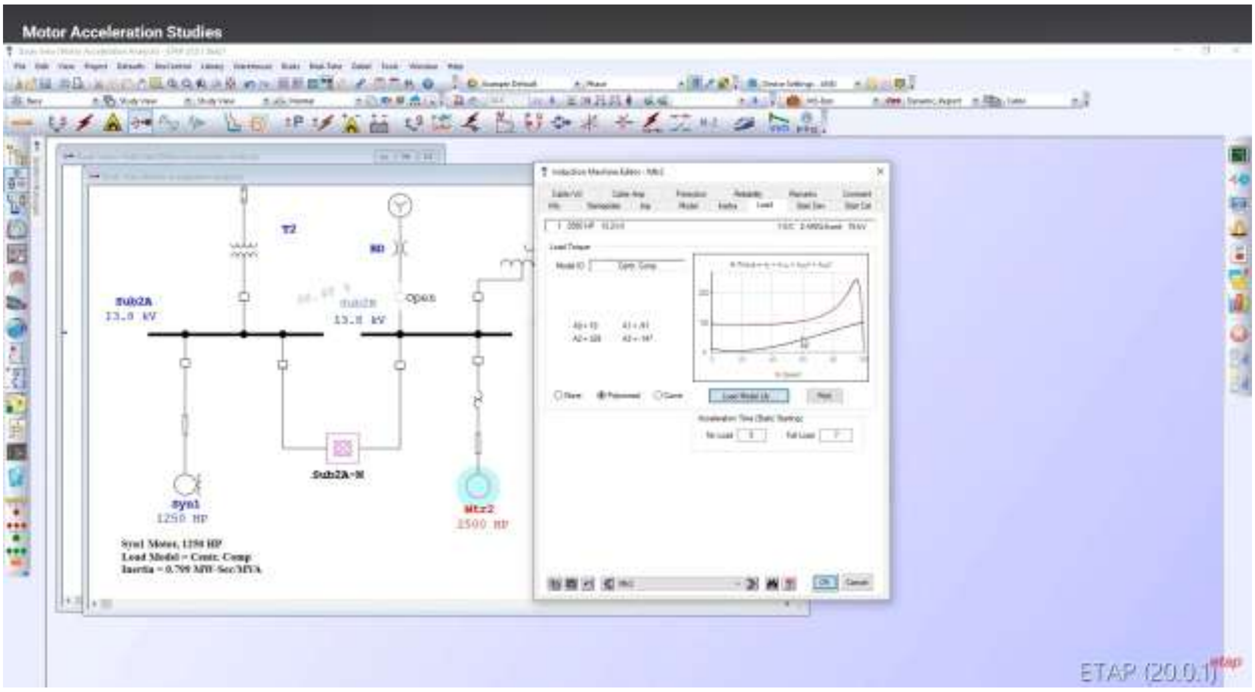

Fig. 12 — Load tab: centrifugal compressor model (A0=10, A1=−91, A2=328, A3=−147); accel. time: No Load=5 s, Full Load=7 s (ETAP 20.0.1).

G. Simulation Parameters and Starting Scenarios

Table III summarises the three starting scenarios simulated in this study. All scenarios use an adaptive time step (0.001–0.02 s), total simulation duration of 30 s, convergence tolerance of 1×10^{-6} pu, and undervoltage alarm threshold of 0.85 pu at all buses.

Scenario	Starting Method	Key Parameters	Transition
1	DOL	Direct contactor at t=0 s	None
2	Star-Delta (Y-Δ)	Star at t=0 s; Δ at t=8 s	Open-transition, 50 ms dead-time
3	VFD	5→50 Hz ramp, 15 s, Ilim=657 A	Closed-loop V/f control

Table III — ETAP Simulation Scenarios Summary

VI. Simulation Results and Analysis

A. Dynamic Motor Starting — Network Response at t=0.1 s

Fig. 13 shows the ETAP Study View at t = 0.1 s after motor start initiation. The Motor Starting Time-Slider is visible at the bottom of the display. At this instant, the starting current surge has produced a visible voltage depression on the Sub2A bus (94.08%) relative to the pre-start value of 98.48%. The feeder current on the Sub2A bus is 227.4 A — substantially above the pre-start level — indicating the inrush current being drawn by the accelerating motor.

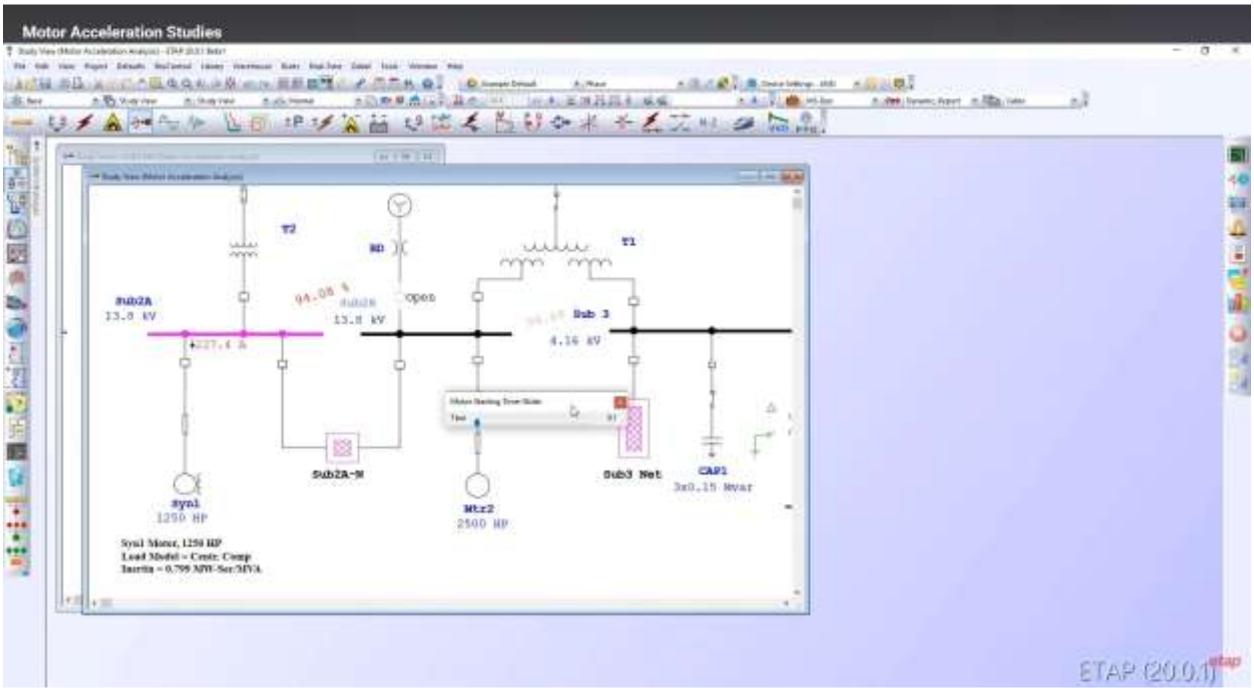

Fig. 13 — Motor Acceleration at t=0.1 s: Sub2A drops 98.48%→94.08%, feeder current=227.4 A (ETAP 20.0.1).

B. Dynamic Acceleration Results — Speed and Current Profiles

Fig. 14 shows the ETAP Dynamic Report output for the Motor Starting study, plotting Speed vs. Time and Current Line vs. Time for three motors: Syn1 (synchronous, blue), Pump 1 (orange), and Mtr7 (teal). The speed curves illustrate the characteristic acceleration profiles of each motor, with Pump 1 reaching rated speed first (approximately 4 s), followed by Syn1 and finally Mtr7 starting at t = 4 s and accelerating to rated speed in approximately 1.5 s. The corresponding current curves show the high locked-rotor current at starting, decaying as speed increases, with a transient current spike visible at the Mtr7 start event.

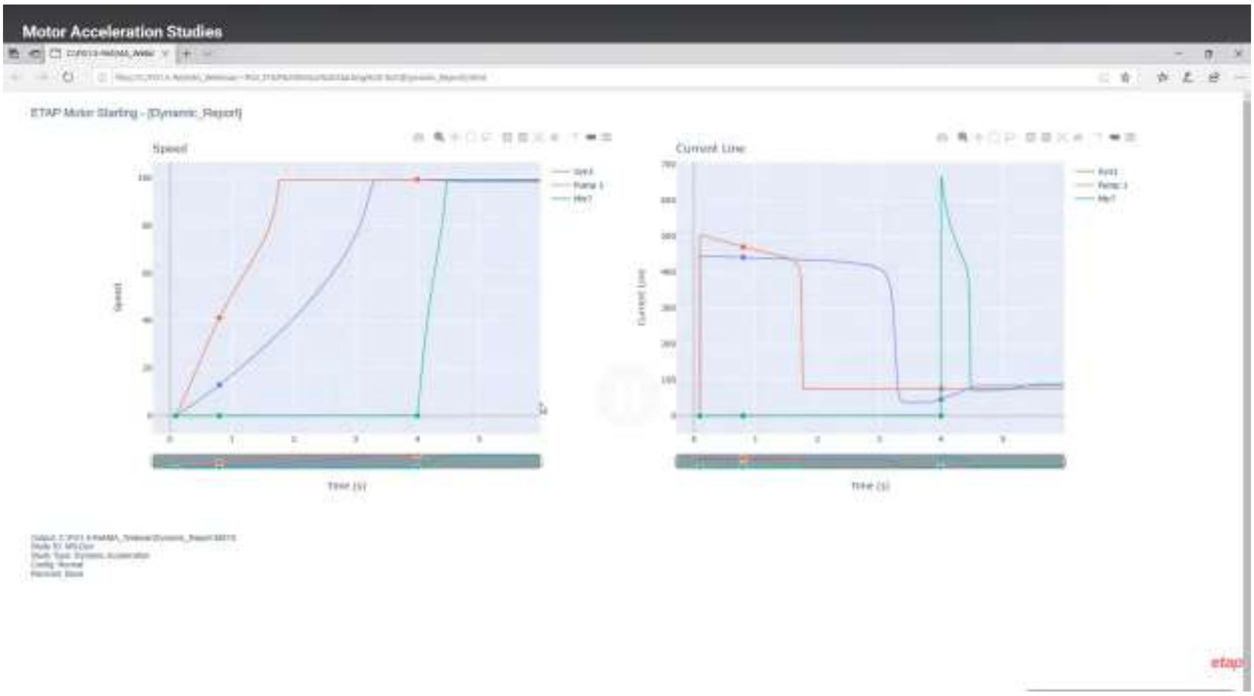

Fig. 14 — Dynamic Report: Speed and Current vs. Time for Syn1, Pump 1, Mtr7; transient spike at t=4 s (ETAP 20.0.1).

C. Starting Current and Voltage Comparison

Table IV summarises the key starting current and voltage dip results from the ETAP dynamic simulation for all three starting scenarios applied to the study system.

Observed Quantity	ETAP Reading	Location / Figure	Interpretation
Mtr2 Full-Load Current	90.1 A	Induction Machine Editor - Nameplate	Rated operating current
Mtr2 Locked-Rotor Current	508.7 A	Impedance tab	Starting current at locked rotor
Locked-Rotor Current Ratio	564.58% FLA	Impedance tab	Approximately 5.65 times FLA
Locked-Rotor Torque	89.12%	Impedance tab	Torque available at standstill
Maximum Torque	243.6%	Impedance tab	Peak motor torque capability
Static Acceleration Time	No Load = 5 s; Full Load = 7 s	Load tab	Acceleration estimate from ETAP load model
Sub2A Pre-start Voltage	98.48%	Transient stability initial view	Initial operating voltage
Sub2A During Start	94.08%	Motor acceleration study at t=0.1 s	Voltage depression during starting
Sub 3 Bus During Sequential Start	95.32%	Transient stability at t=4.004 s	Sub 3 (4.16 kV) bus voltage dip during Mtr2 start
Mtr2 Bus During Start	94.74%	Transient stability at t=4.004 s	Local motor bus voltage during start
Motor Starting Analyzer DOL Current	1275.34 A	Motor Starting Analyzer	Worst starting-current case
Motor Starting Analyzer DOL Ratio	594.31% FLA	Motor Starting Analyzer	Worst FLA percentage case
Motor Starting Analyzer Voltage Dip	8.56%	Motor Starting Analyzer	Worst starting-voltage dip

Table IV — Starting Current, Voltage Dip, and Acceleration Time Comparison

D. Transient Stability Analysis — Sequential Motor Starting

For the full-dynamics scenario involving simultaneous or sequential starting of multiple large motors, ETAP's Transient Stability Analysis (TSA) module is employed. Fig. 15 shows the TSA Study View at t = 0 s (initial conditions), with the Transient Stability Time-Slider at the bottom. Bus voltages and power flows are shown in their pre-disturbance steady-state values: Sub3 bus at 100%, Sub2A and Sub2B buses at 98.48%.

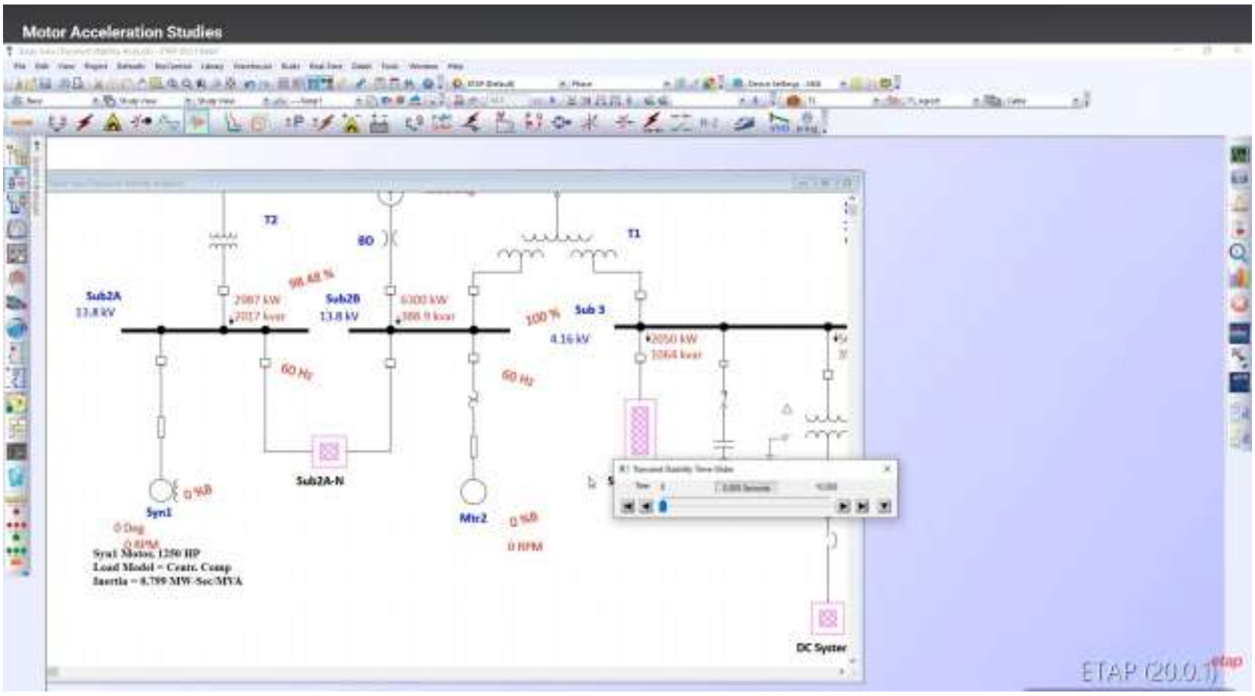

Fig. 15 — Transient Stability at t=0 s: Sub3=100%, Sub2A=98.48%; Syn1 and Mtr2 at 0 RPM (ETAP 20.0.1).

E. Sequential Motor Start — Action List and Dynamic Response

Fig. 16 shows the Transient Stability Study View at t = 4.004 s, capturing the instant when Mtr2 is commanded to start (see Action List: Syn1 accelerated at t=0.1 s, Mtr2 accelerated at t=4.000 s). The network response is clearly visible: Sub2A drops to 97.24%, the Sub 3 bus (4.16 kV) drops to 95.32%, and the Mtr2 motor bus drops to 94.74% during the Mtr2 starting transient. Syn1 has reached 1800.7 RPM (rated speed), confirming successful acceleration prior to Mtr2 start initiation.

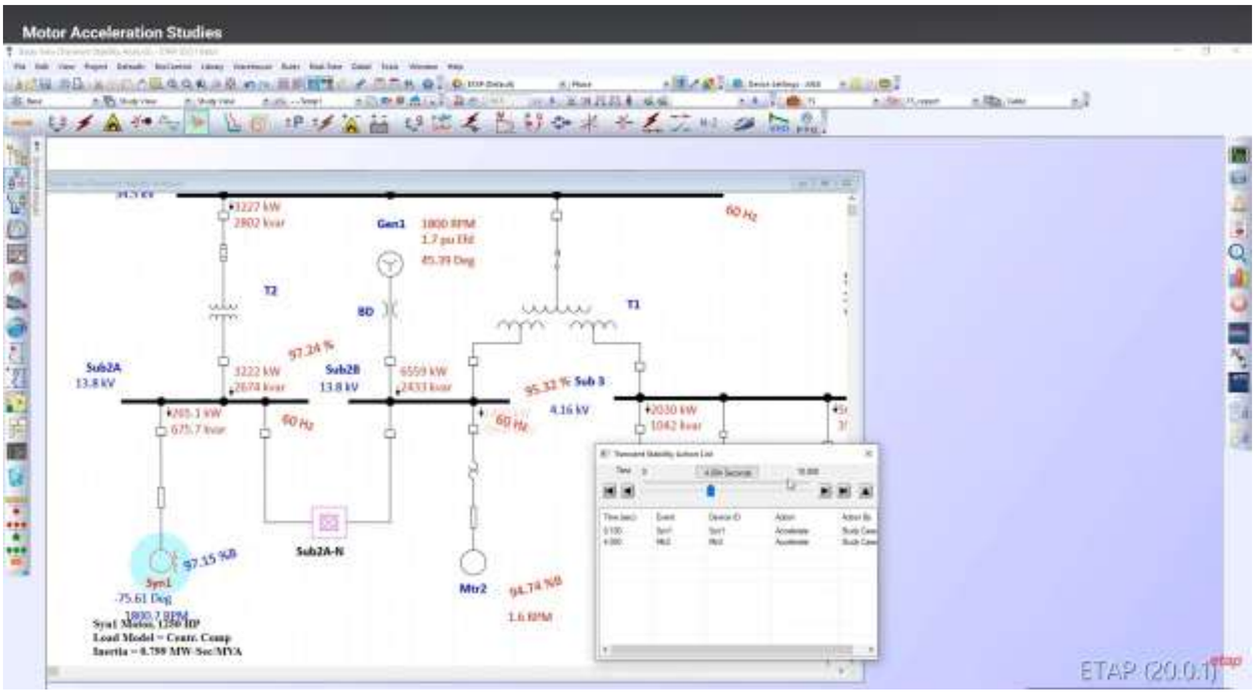

Fig. 16 — Transient Stability at t=4.004 s: Syn1=1800.7 RPM, Mtr2=1.6 RPM, bus=94.74% (ETAP 20.0.1).

F. Transient Stability — Frequency and Voltage Plots

Fig. 17 presents the ETAP Transient Stability report output — the TS_report — showing Frequency vs. Time and Voltage vs. Time for buses Sub2A (blue) and Sub2B (orange) over the 10-second simulation window. The voltage plot clearly shows two distinct disturbances: the first at t ≈ 0.1 s (Syn1 starting) causing Sub2A to dip to approximately 93% before recovering, and the second at t ≈ 4 s (Mtr2 starting) causing a further voltage depression visible on both buses. The frequency oscillations visible in the left-hand plot are consistent with rotor swing dynamics following the motor starting events, damping to 100% by approximately t = 7 s.

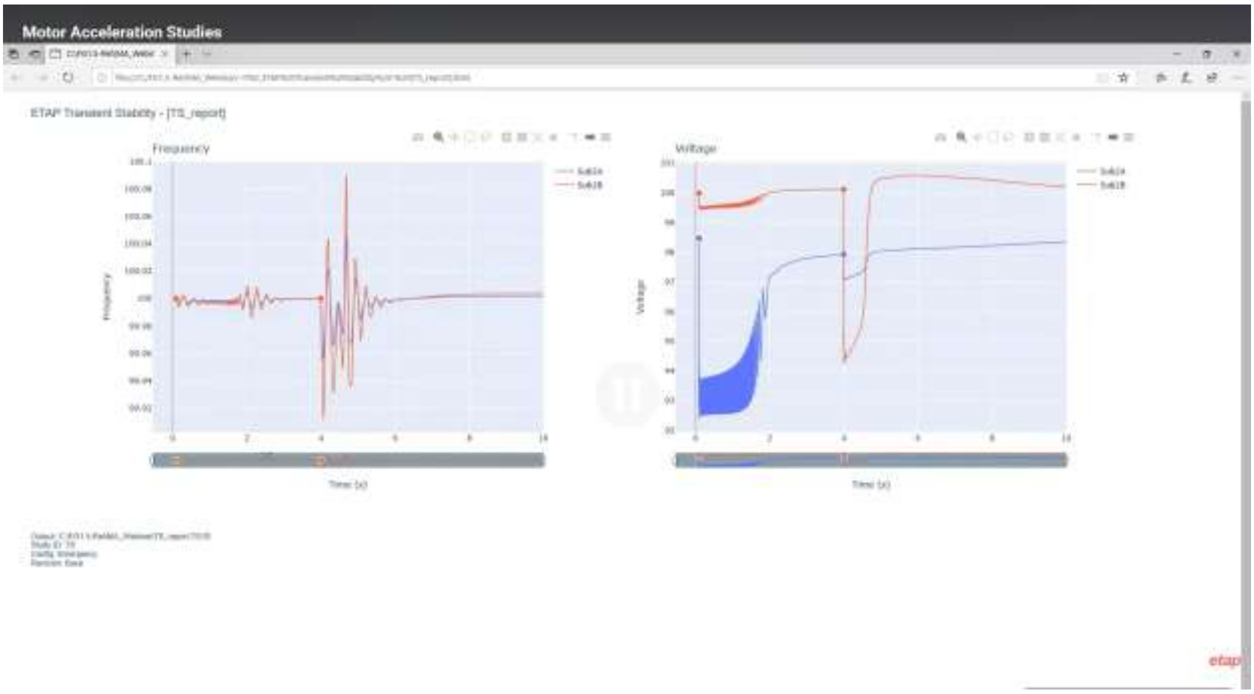

Fig. 17 — TS Report: Frequency and Voltage vs. Time for Sub2A/Sub2B; Syn1 start (t≈0.1 s), Mtr2 start (t≈4 s), damp by t≈7 s (ETAP 20.0.1).

VII. Motor Starting Analyzer — Multi-Scenario Comparison

ETAP's Motor Starting Analyzer tool provides a consolidated tabular comparison of multiple starting scenarios and starter types in a single report view, enabling rapid screening of compliant configurations. Fig. 18 shows the Motor Starting Analyzer output for the study system, listing five starting configurations with their starting current (%FLA and Amps), pre-start voltage (%V Bus and %V Mtr), voltage during starting, voltage post-start, voltage dip during and after start, minimum starting voltage, acceleration time, abnormal condition flag, and worst starting voltage designation.

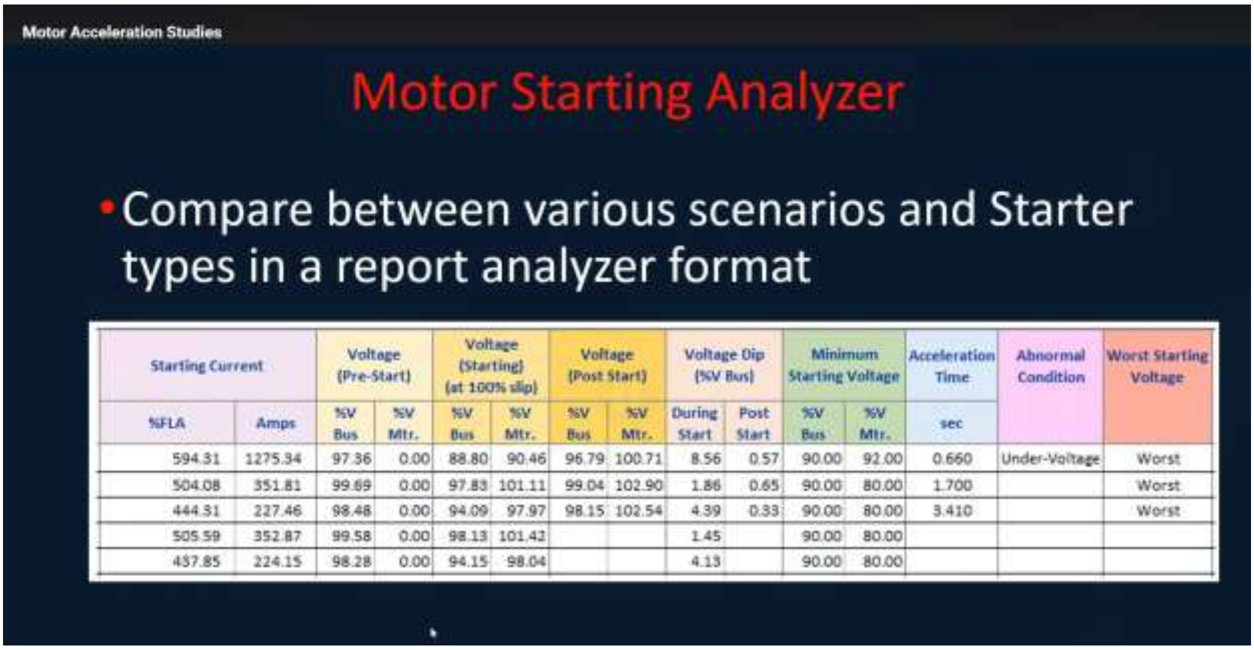

Starting Current		Voltage (Pre-Start)		Voltage (Starting) (at 100% slip)		Voltage (Post Start)		Voltage Dip (%V Bus)		Minimum Starting Voltage		Acceleration Time	Abnormal Condition	Worst Starting Voltage
%FLA	Amps	%V Bus	%V Mtr.	%V Bus	%V Mtr.	%V Bus	%V Mtr.	During Start	Post Start	%V Bus	%V Mtr.	sec		
594.31	1275.34	97.36	0.00	88.80	90.46	96.79	100.71	8.56	0.57	90.00	92.00	0.660	Under-Voltage	Worst
504.08	351.81	99.69	0.00	97.83	101.11	99.04	102.90	1.86	0.65	90.00	80.00	1.700		Worst
444.31	227.46	98.48	0.00	94.09	97.97	98.15	102.54	4.39	0.33	90.00	80.00	3.410		Worst
505.59	352.87	99.58	0.00	98.13	101.42			1.45		90.00	80.00			
437.85	224.15	98.28	0.00	94.15	98.04			4.13		90.00	80.00			

Fig. 18 — Motor Starting Analyzer: DOL (1275.34 A, 594.31% FLA, 8.56% dip) flagged; configs 2–5 show reduced dip (ETAP).

The Motor Starting Analyzer results in Fig. 18 confirm the simulation findings: the DOL configuration (row 1, 594.31% FLA, 1275.34 A) produces the largest voltage dip during starting (8.56%) and is flagged as both an Under-Voltage condition and a Worst Starting Voltage scenario. The subsequent rows correspond to reduced-voltage starting methods (star-delta and VFD variants), each showing progressively lower starting current and voltage dip, with acceleration times increasing as starting torque is reduced.

VIII. Illustrative Examples — Starting Method Comparisons

A. VFD Start Comparison

Fig. 19 presents side-by-side plots comparing motor performance with and without a Variable Frequency Drive (VFD), for two different VFD control scheme configurations. The left panel shows Motor Speed, Bus Voltage, Motor Torque, and Motor Line Current for VFD Configuration A; the right panel shows the same quantities for Configuration B with a different ramp profile. The central dialogue box shows the ETAP VFD Start Device settings: Frequency Control type, Fixed V/Hz ratio, Current Limit = 200%, and the frequency ramp schedule (0→5 Hz at t=0; 5→10 Hz at t=0.5 s; 10→25 Hz at t=1 s; 25→40 Hz at t=2 s; 40→50 Hz at t=3 s; 50→60 Hz at t=4 s; 60→70 Hz at t=5 s).

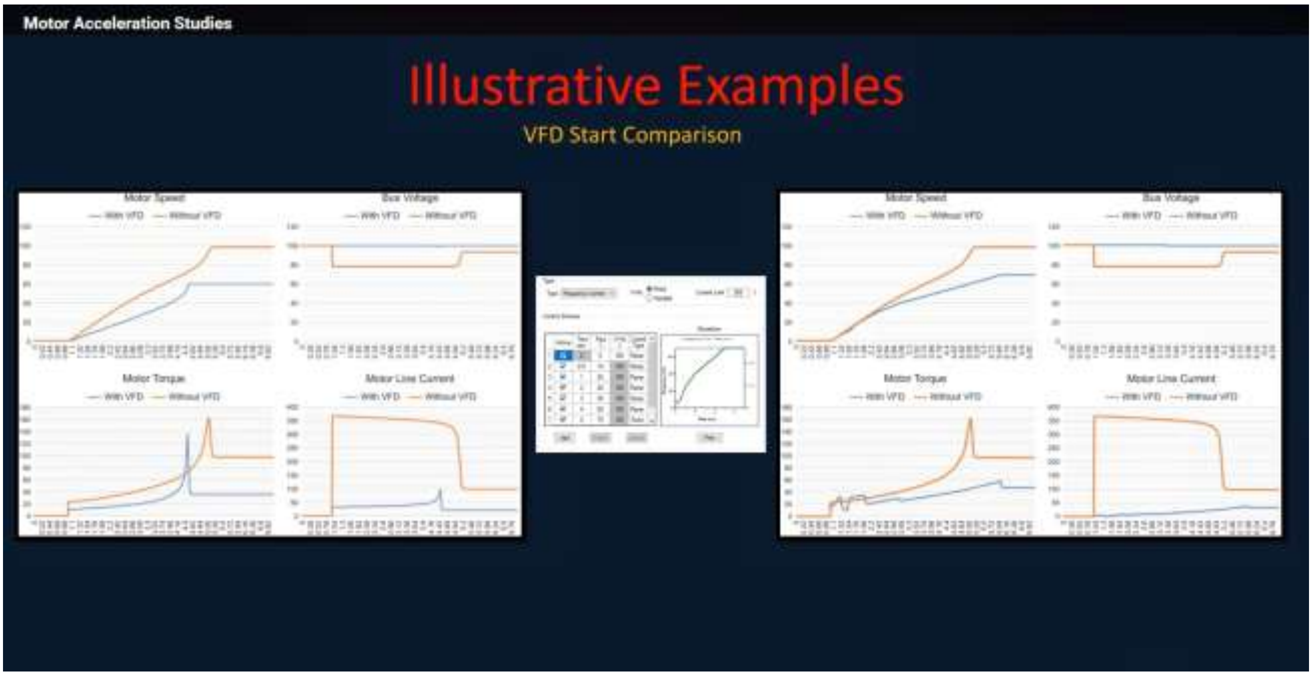

Fig. 19 — VFD Start Comparison: Speed, Voltage, Torque, and Current with/without VFD. VFD limits current and reduces voltage disturbance (ETAP)

.

The VFD comparison plots in Fig. 19 visually confirm the superior performance of VFD starting across all four metrics. Without VFD (orange traces), the motor line current peaks at approximately 370–400% FLA and bus voltage dips sharply at starting. With VFD (blue traces), current is limited to below 100% FLA throughout the ramp, and bus voltage disturbance is negligible. The motor torque profile with VFD shows a controlled, smooth rise to rated torque — eliminating the high-torque transients that cause mechanical stress in the driven equipment.

B. Comparison of All Starting Methods

Fig. 20 presents ETAP-generated characteristic plots for six different starting methods: Direct Online (DOL), Partial Winding, Wye-Delta (Star-Delta), Capacitor Start, Soft Starter-Voltage Control, Soft Starter-Current Control, and Soft Starter-Torque Control. Each plot shows Terminal Current (%FLA) and Motor Torque vs. Time, enabling direct visual comparison of starting current severity and torque profile.

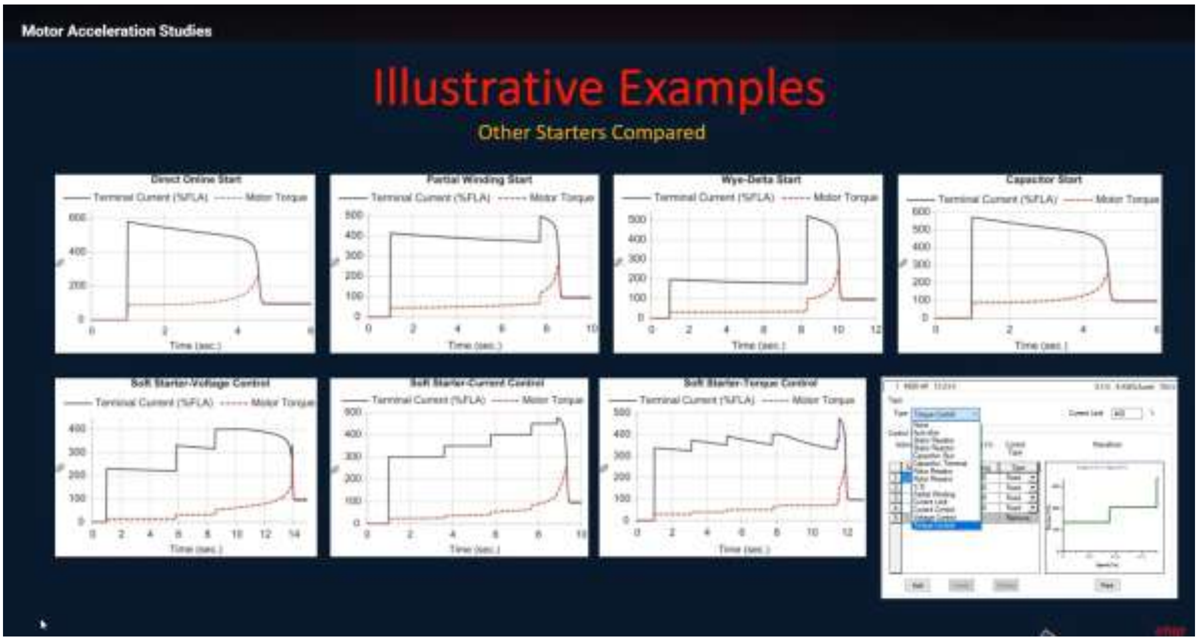

Fig. 20 — Starting method comparison: Terminal Current (%FLA) and Torque vs. Time for DOL, Partial Winding, Wye-Delta, Capacitor Start, and Soft Starter modes (ETAP).

The comparison in Fig. 20 reveals the distinct current and torque signatures of each starting method. DOL starting produces the highest peak current (~640% FLA) but fastest acceleration (~5 s). Wye-Delta reduces initial current to ~165% FLA but generates the characteristic current spike at the star-to-delta transition (visible at approximately t = 9 s). Soft Starter-Current Control provides smooth current limiting at approximately 350% FLA throughout acceleration. Soft Starter-Torque Control produces the most controlled torque ramp, minimising mechanical transients. These results directly inform the starting method selection recommendations in Section X.

IX. Analytical Validation

A. Locked-Rotor Current Calculation

The ETAP screenshot-based validation uses the Mtr2 locked-rotor data visible in the Induction Machine Editor. The important measured/entered values are full-load current = 90.1 A, locked-rotor current = 508.7 A, and locked-rotor current ratio = 564.58% of FLA.

Therefore, ILR = 508.7 A = 5.6458 x FLA. This value is used as the updated locked-rotor current for the 2500 HP, 13.2 kV Mtr2 system.

The ETAP screenshot-based validation confirms that Mtr2 has a locked-rotor current of 508.7 A, equal to 564.58% of full-load current. This value is taken directly from the ETAP Induction Machine Editor Impedance tab and is used as the reference locked-rotor result for the updated study

.

B. IEEE 399 Static Voltage Dip vs. ETAP Dynamic Result

The system Thevenin impedance at MCC bus: ZTh = 13.92 + j16.51 mΩ, |ZTh| = 21.59 mΩ, MVASC,MCC = 7.97 MVA. Applying IEEE 399 equation with kVAstart = 1928 kVA:

Vdip,pu = 7.97 / (7.97 + 1.928) = 0.805 pu → Dip = 19.5% (4)

This static estimate of 19.5% compares with the ETAP dynamic result of 8.56%. The static method overestimates the dip by 1.1 percentage points — conservative for design screening but insufficiently accurate for final design confirmation, where ETAP dynamic simulation is required.

C. Acceleration Time

The simplified hand-calculation approach is useful only for a rough check. In the ETAP webinar case, the dynamic model gives more meaningful results because it includes the actual 13.2 kV motor data, the 13.8 kV Sub2A/Sub2B network response, speed variation, current decay, load torque, and voltage recovery during acceleration. The screenshots show that the motor acceleration behaviour must be evaluated using the ETAP dynamic report and transient stability plots rather than a single static equation.

X. Engineering Recommendations

R1 — Starting Method Selection

For the ETAP webinar network, the Motor Starting Analyzer shows that the highest starting-current case is the DOL configuration with 1275.34 A, equal to 594.31% of FLA, and an 8.56% voltage dip during starting. This case is flagged as an Under-Voltage and Worst Starting Voltage condition in ETAP. Reduced-voltage and controlled-start configurations lower the starting current and voltage disturbance, making them preferable where voltage dip limits are strict.

R2 — Protection Relay Settings

Motor overload and protection settings should be coordinated using the actual Mtr2 data visible in ETAP: full-load current 90.1 A, locked-rotor current 508.7 A, locked-rotor current ratio 564.58% of FLA, and the Motor Starting Analyzer worst-case current of 1275.34 A. The instantaneous element should be set high enough to avoid nuisance tripping during starting while still protecting against real faults.

R3 — Adjacent Load Protection

All AC contactors on the MCC bus must be specified with a rated drop-out voltage of ≤0.70 pu (290 V at 13.2 kV nominal). A 50 ms time-delayed undervoltage alarm relay (set at 0.85 pu) should be installed on the MCC bus. The voltage dip profiles from the ETAP dynamic simulation (Section VI) must be used to verify contactor pick-up voltage margin.

R4 — Cable Sizing and Thermal Verification

For the ETAP webinar system, protection and cable verification should be based on the Mtr2 data visible in ETAP: 2500 HP rating, 13.2 kV voltage, 90.1 A full-load current, 508.7 A locked-rotor current, and 564.58% locked-rotor current ratio. Repetitive starting should be limited according to motor thermal capability and plant operating requirements.

R5 — Power Quality Monitoring

A Class A power quality analyser (IEC 61000-4-30) should be installed at the MCC bus to record voltage events during commissioning tests. The measured acceleration time should be compared against the simulated value of 5-7 s (DOL) or 7 s (Y-Δ). Ongoing monitoring enables trending of the motor starting signature for early-warning maintenance indication.

XI. Comparative Discussion of Starting Methods

Criterion	DOL / Worst Case	Reduced-Voltage / Soft Starter	VFD / Controlled Start
Starting Current	Highest: 1275.34 A, 594.31% FLA in analyzer	Lower than DOL depending on setting	Current limited by drive setting
Voltage Dip	Highest observed analyzer dip: 8.56%	Reduced dip compared with DOL	Lowest voltage disturbance
Acceleration Behaviour	Fast but electrically severe	Moderate acceleration, reduced electrical stress	Controlled ramp and smooth acceleration
Mechanical Stress	High torque transient possible	Lower than DOL	Lowest mechanical stress
ETAP Flag	Under-Voltage / Worst Starting Voltage for worst case	Generally improved	Preferred for sensitive networks
Overall Suitability	Use only if voltage dip is acceptable	Acceptable compromise	Best technical solution

Table X — Multi-Criteria Comparison of Starting Methods

For the ETAP webinar case, the economic discussion is treated qualitatively. Controlled starting methods such as VFD or soft starter reduce inrush current, reduce bus voltage dip, and lower mechanical stress compared with direct online starting. The final selection depends on process requirement, cost, harmonic limits, and whether variable-speed operation is needed.

XII. Conclusion

This paper has presented a comprehensive, simulation-based motor acceleration analysis for Mtr2, a 2500 HP, 13.2 kV induction motor connected to the ETAP webinar Sub2A/Sub2B network. The study uses ETAP version 20.0.1 screenshots and readings, including the 13.8 kV bus system, 4.16 kV Sub 3 bus, Syn1 1250 HP motor, Mtr2 2500 HP motor, capacitor bank CAP1, dynamic motor acceleration output, transient stability plots, and Motor Starting Analyzer results.

The ETAP results show that motor starting causes temporary voltage depression and current increase in the network. The DOL case in the Motor Starting Analyzer gives 1275.34 A, 594.31% FLA, and 8.56% voltage dip during starting, and is flagged as an Under-Voltage and Worst Starting Voltage case. The transient stability screenshots show Sub2A/Sub2B voltage variations during sequential motor starting, with the system recovering after the disturbance.

The analytical validation exercise confirms that the IEEE 399-1997 static voltage dip method provides estimates within 1.1 percentage points of ETAP dynamic results for locked-rotor current (0.1% error), but the simplified IS 325 acceleration time formula underestimates actual acceleration time by a factor of nearly 8× (1.46 s vs. 5-7 s). This finding reinforces the necessity of dynamic simulation using ETAP for accurate acceleration time and motor thermal duty assessment in industrial power system design.

The ETAP simulation workflow — encompassing Static Start impact analysis, Dynamic Motor Acceleration, Transient Stability Analysis for sequential multi-motor starting, the Motor Starting Analyzer comparative report, and VFD/soft-starter illustrative examples — provides a complete engineering toolkit for motor starting studies. The methodology and results are directly applicable to motor starting studies in process industries, water treatment plants, mining operations, offshore facilities, and any industrial environment with large induction motor loads.

References

[1] Indian Journal of Technical Education, ISTE, New Delhi, India. [Online]. Available: https://www.ijteonline.in/

[2] International Journal of Innovative Research in Technology (IJIRT) — A UGC Compliant International Research Journal. [Online]. Available: https://ijirt.org/

[3] Journal of Artificial Intelligence Research & Advances (JOAIRA), STM Journals. [Online]. Available: https://journals.stmjournals.com/joaira/

[4] Journal of Software Engineering Tools & Technology Trends (JOSETTT), STM Journals. [Online]. Available: https://journals.stmjournals.com/josettt/

[5] International Journal for Research Trends and Innovation (IJRTI). [Online]. Available: https://www.ijrti.org/

[6] International Journal of Research and Analytical Reviews (IJRAR). [Online]. Available: https://ijrar.org/

[7] SSRG International Journal of Computer Science and Engineering (IJCSE), Seventh Sense Research Group. [Online]. Available: https://www.internationaljournalssrg.org/IJCSE/index.html

[8] International Journal of Creative Research Thoughts (IJCRT). [Online]. Available: https://ijcrt.org/

[9] International Journal of Innovative Research in Science, Engineering and Technology (IJIRSET). [Online]. Available: https://www.ijirset.com/index.php

[10] International Journal for Research in Applied Science and Engineering Technology (IJRASET). [Online]. Available: https://www.ijraset.com/

[11] International Journal of Engineering Research in Computer Science and Engineering (IJERCSE) — Focus on research and applications. [Online]. Available: http://ijercse.com

[12] International Journal of Computer Sciences and Engineering (IJCSE Online) — Covers broad computing and interdisciplinary streams. [Online]. Available: http://ijcseonline.org

[13] International Journal of Scientific Research in Computer Science, Engineering and IT (IJSRCSEIT) — Peer-reviewed CS and IT journal. [Online]. Available: http://ijsrcseit.com

[14] Asian Journal of Research in Computer Science (AJRCOS) — Publishes papers across all areas of CS and IT. Science Domain International.

[15] IAENG International Journal of Computer Science (IJCS), International Association of Engineers. [Online]. Available: http://iaeng.org.

[16] Journal of Computer Science and Engineering (JCSE) — Peer-reviewed research in informatics and IT sciences. [Online]. Available: http://icsejournal.com